European Cells and Materials Vol. 35 2018 (pages 13-24) DOI: 10.22203/eCM.v035a02 ISSN 1473-2262

TiO_2 NANOPARTICLES CAN SELECTIVELY BIND CXCL8 IMPACTING ON NEUTROPHIL CHEMOTAXIS

J. Batt[1], M. Milward[1], I. Chapple[1], M. Grant[1], H. Roberts[2] and O. Addison[1,2,*]

[1] School of Dentistry, University of Birmingham, Birmingham, United Kingdom
[2] School of Dentistry, University of Alberta, Edmonton, Alberta, Canada

Abstract

The interaction between TiO_2 nanoparticles (NPs) and inflammatory cytokines, including CXCL8, a clinically relevant pro-inflammatory chemokine, was investigated. TiO_2 is present in tissues adjacent to failing implanted Ti (titanium) devices. TiO_2 NPs were shown to bind to CXCL8 *in vitro*, causing perturbation of quantification of CXCL8 by ELISA, in both simple and complex protein panels, in a dose-dependent manner. Binding between TiO_2 NPs and CXCL8 was demonstrated by protein gel electrophoresis. TiO_2 NPs were also shown to inactivate the chemoattractant property of CXCL8 in a dose-dependent manner, suggesting that the binding between TiO_2 NPs and CXCL8 is likely to be clinically relevant. The results of this study disputed the applicability of detection of CXCL8 by ELISA in systems where TiO_2 NPs were present. Clinically, the disruption of neutrophil chemotaxis due to CXCL8 binding to TiO_2 NPs might result in a hampered inflammatory response.

Keywords: Titanium dioxide, nanoparticles, cytokines, chemokines, neutrophils, chemotaxis.

*Address for correspondence: Owen Addison, School of Dentistry, University of Alberta, Edmonton, T6G 1C9, Canada.
Telephone: +1 7804925308 Email: oaddison@ualberta.ca

Introduction

Humans are exposed to nanoparticles (NPs) from a wide variety of sources and through a broad range of exposure routes. Consequently, considerable attention is given to both the potential hazards of NP exposures (Chan *et al.*, 2011; Jin *et al.*, 2011; Shukla *et al.*, 2011; Yazdi *et al.*, 2010) and also, contrastingly, to their therapeutic use (Holpuch *et al.*, 2010; Zhang and Monteiro-Riviere, 2013). Many studies concerning the toxicology of NPs and their interactions with a wide range of tissues and cells continue to be reported. However, the modelling of NP exposures to tissues is complex, given the propensity for NP aggregation (Zhang, 2014) and for the NPs to strongly adsorb biomolecules to their surfaces (Xia *et al.*, 2011). Consequently, at the cellular level, interactions are often with the NP surface biomolecule corona and not the particle itself (Tenzer *et al.*, 2013). The ability of certain NPs to strongly adsorb soluble biomolecules also has implications for cell-to-cell signalling and it is conceivable that, whilst certain NPs may not be directly cytotoxic, they have the ability to subtly alter the composition (concentration and concentration gradient) of biomolecules in extracellular environments. How titanium (Ti) NPs may exert such indirect effects through perturbation of cell-to-cell signalling processes was explored using TiO_2 NPs. TiO_2 can be found in tissues surrounding implanted Ti devices associated with peri-prosthetic inflammation, likely in NP form (Addison *et al.*, 2012). They are contained in many consumer products, such as cosmetics and sunscreens (Frohlich and Roblegg, 2012), and are advocated for a variety of biomedical applications, such as drug delivery systems, cancer treatments and cell imaging techniques (Yin *et al.*, 2013).

Biological responses to TiO_2 surfaces have been studied in detail and are shown to be both favourable and predictable [presenting minimal immune cell activation and promoting favourable responses from structural cells, such as surface adhesion and cell proliferation (Lu *et al.*, 2008)]. However, when TiO_2 is reduced to ultrafine and nano-scale forms, very different cellular responses are reported (Silva *et al.*, 2013). Potential exposure routes to TiO_2 NPs include inhalation, absorption through dermal and mucous membranes and particles generated *in situ* around implanted devices (Addison *et al.*, 2012; Frohlich and Roblegg, 2012; Tucci *et al.*, 2013). TiO_2 NPs are shown to be directly toxic to epithelial cells in *in vitro* models (Gerloff *et al.*, 2012; Gurr *et al.*, 2005; Kocbek *et al.*, 2010; Park *et al.*, 2008; Singh *et al.*, 2007; Srivastava *et al.*, 2013) and to induce pulmonary inflammation in rodent models, following inhalational exposure (Bonner *et al.*, 2013; Kobayashi

et al., 2009). Absorption of TiO_2 NPs through the gastrointestinal mucosa is also demonstrated in animal models (Brun *et al.*, 2014; Jani *et al.*, 1990; Jani *et al.*, 1994), leading to transmucosal distribution and cellular internalisation. In contrast to these findings, the toxicological effects of intravascular injected TiO_2 NPs are minimal and the majority of particles (92 %) localise to the liver 24 h post-infusion (Elgrabli *et al.*, 2015). Generation of a range of Ti species (including metallic and oxide NP forms) *in situ* is also shown in areas adjacent to implanted Ti prostheses and these products are presumed to subsequently interact with innate and acquired immune cell populations (Addison *et al.*, 2012; Cadosch *et al.*, 2009; Jonas *et al.*, 2001, Olmedo *et al.*, 2008, Torgersen *et al.*, 1995). TiO_2 NPs can be pro-inflammatory, increasing the production of pro-inflammatory cytokines and chemokines (herein referred to as inflammatory mediators), such as interleukin-8 (IL-8, also known as CXCL8) in mesenchymal and epithelial cells (Haleem-Smith *et al.*, 2012; Wilson *et al.*, 2000) and tumour necrosis factor alpha (TNFα) and receptor activator of nuclear factor kappa-B (RANKL) in fibroblasts (Irshad *et al.*, 2013; Qian *et al.*, 2013). Biological responses are sensitive to particle size, speciation and morphology (Singh *et al.*, 2007) and, whilst the direct cellular effects of TiO_2 NPs have been investigated extensively, there is a paucity of data exploring the biological effects of TiO_2 NPs within the extracellular environment.

NPs possess high surface energy favouring biomolecular adsorption (Horie *et al.*, 2013) and, whilst this is recognised in the literature, the impact on data interpretation from NP exposure assays is frequently underestimated or ignored (Kroll *et al.*, 2009). Where NPs are shown to induce or fail to induce cytokine expression measured by ELISAs, it is important to recognise that the assay result will be affected by any binding between the NPs and inflammatory mediators or components of the assay system (Irshad *et al.*, 2013). Despite the plethora of data reported, few studies have acknowledged this issue. The presence of NPs within an ELISA system can result in adsorption of inflammatory mediators, as reported for carbon NPs adsorbing CXCL8 (Hsiao and Huang, 2011; Monteiro-Riviere and Inman, 2006) and TiO_2 NPs adsorbing interleukin-6 (IL-6) (Veranth *et al.*, 2007).

Exposure to TiO_2 NPs can stimulate the release of CXCL8 (as identified by ELISA) from a variety of cell types, including human endothelial cells (Peters *et al.*, 2004) and human lung epithelial cells (Wilson *et al.*, 2012). CXCL8 is a pro-inflammatory chemokine and a potent chemoattractant produced by a variety of cell types, specifically targeting neutrophils (Bickel, 1993). Therefore, CXCL8 is a key factor in the initiation and propagation of the inflammatory response. Other studies use ELISA techniques to identify CXCL8 release in a context where TiO_2 NPs are present, with no mention of the potential for CXCL8 depletion by the presence of TiO_2 NPs (Peters *et al.*, 2004; Singh *et al.*, 2007).

The aim of this study was to investigate how extracellular TiO_2 NPs interact with a selection of inflammatory mediators involved in cell-to-cell signalling [CXCL8, TNFα, interleukin 1-beta (IL1-β), IL-6, interferon-gamma (IFN-γ)] during inflammation, with specific emphasis on CXCL8 and human neutrophil or polymorphonuclear leukocyte (PMNL) chemotaxis. The effects of the presence of TiO_2 NPs within an ELISA detection system on these inflammatory mediators was also established. Given the lack of previously reported evidence, our null hypothesis was that the presence of TiO_2 NPs had no selective impact on the adsorption of extracellular inflammatory mediators.

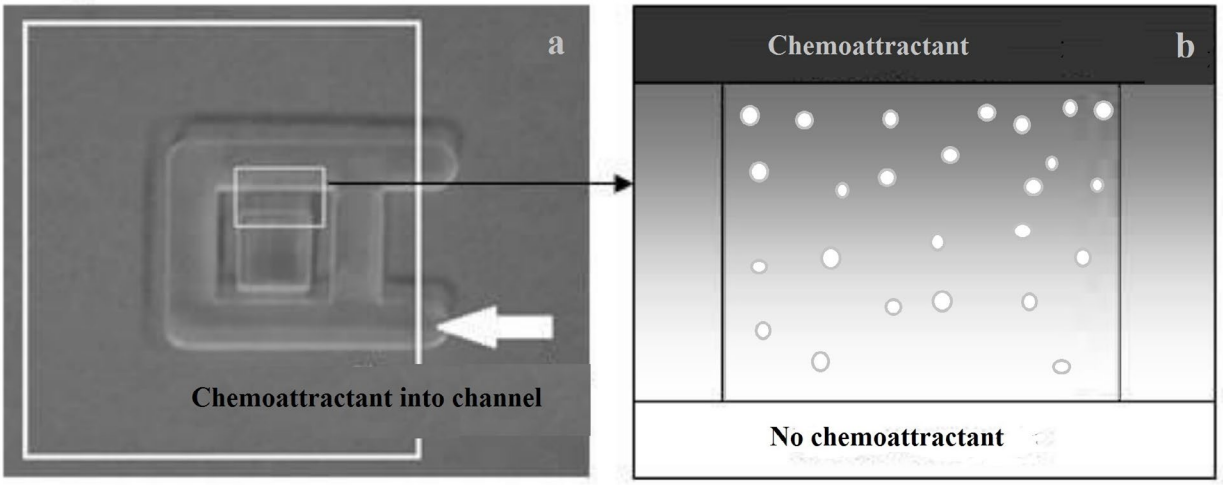

Fig. 1. (**a**) Optical image and (**b**) schematic illustration of the "bridge" of the Insall chamber. (**a**) The image shows the channels scribed into the chamber and the position of the coverslip, represented by the large white rectangle. The inset rectangle shows the detail of the "bridge" area of the chamber, where a gradient of chemoattractant is formed. This area of the chamber is visualised throughout the assay.

Materials and Methods

TiO_2 NP (stimulus) preparation

TiO_2 (powder, anatase form, purity 99.7 %, catalogue number 637254, Sigma-Aldrich, Gillingham, UK) in the form of nanoparticles with a particle size < 25 nm was selected. The powder was heat-treated at 200 °C for 30 min to minimise endotoxin contamination. TiO_2 was added to sterile ultrapure water at mixing ratios of 0.05, 0.5 and 5 g in 50 mL of H_2O to provide a stock concentration of 100, 1000 and 10000 μg/mL. The TiO_2 NP suspension was placed on ice and sonicated using a Branson Sonifier 250 (Branson Ultrasonics, Danbury, CT, USA) according to the protocol described by Taurozzi *et al.*, (2013). Briefly, a "standard ½ inch clean titanium horn" (manufacturer's description) was inserted centrally within a 100 mL beaker to a depth of 10 mm from the base of the vessel. Sonication was performed using a 50 W power output and 80 % duty cycle for 15 min. Sonication was conducted in a positive flow biological hood (MSC12, Thermo Fisher Scientific, Waltham, USA) to maintain aseptic conditions.

Enzyme-linked immunosorbent assays (ELISAs)

ELISAs (CXCL8, IF-γ, IL-1β, TNFα, IL-6) were performed using DuoSet ELISA kits (R&D systems, Bio-techne, Abingdon, UK) according to the manufacturer's instructions. Capture antibodies were diluted in protein-free phosphate-buffered saline (PBS) and 100 μL per well were incubated overnight at room temperature or at 4 °C (target specific) in covered plates, to prevent evaporation or contamination. Then, plates were washed 3 times using PBS containing 0.05 % Tween-20 (Sigma-Aldrich) and the excess blotted using absorbent paper. After washing, wells were blocked with 300 μL of either reagent diluent (RD), comprising 2-amino-2-(hydroxymethyl)propane-1,3-diol (Tris)-buffered saline containing 0.05 % Tween-20 and 0.1 % bovine serum albumin (BSA; Sigma-Aldrich), or blocking buffer (PBS containing 1 % BSA), depending on the target. After 1 h, plates were washed again according to the same washing protocol and then used immediately or stored at 4 °C for no longer than 48 h prior to use. The stated limits of detection from the manufacturer are 31.20-2,000 pg/mL.

Disruption of ELISA assay performance by TiO_2 NPs was assessed. Standards were diluted according to the specific manufacturer's protocols to produce high concentration standards. 100 ppm TiO_2 NPs were added to the high concentration target standard, agitated for 30 s, incubated at room temperature (21 ± 3 °C) for 1 h and centrifuged at 800 ×*g* for 5 min. Following centrifugation, the supernatant was aspirated and serially diluted to produce a panel of standard concentrations. Control standards without TiO_2 NPs were also incubated and centrifuged as above prior to dilution. 100 μL of each sample standard, either containing TiO_2 NPs or not, were added to a prepared well and incubated in a covered plate for 2 h at room temperature. Then, plates were washed 3 times using PBS-Tween-20, as previously described. After washing, streptavidin conjugated to horseradish peroxidase (HRP) was diluted according to the manufacturer's instructions and 100 μL were added to each well and incubated for 20 min in the dark at room temperature. After 20 min, the plates were washed again. 100 μL of a 50 : 50 mix of H_2O_2 and tetramethylbenzidine (TMB) is recommended by the manufacturer; however, in this work a TMB Liquid Substrate System for ELISA (Sigma-Aldrich) was used due to its improved safety profile. The plate was incubated for up to 20 min in the dark as per the manufacturer's instructions. After incubation, 50 μL of 1 M H_2SO_4 were added to each well to stop the reaction and then absorbance was read at 450 nm (absorbance at 570 nm was subtracted to improve accuracy) in a plate reader (ELx800, BioTek, Winooski, VT, USA). To assess variability, ELISA kits from a second manufacturer were used (Abcam ELISA kits for CXCL8, IL-6 and IFN-γ; Abcam, Cambridge, UK). The methodology was similar to the one of the R&D kits and the protocol was followed according to the manufacturer's instruction.

Table 1. A summary of prepared samples for electrophoresis.

No.	Preparation protocol	Sample used
1	2000 pg/mL CXCL8 in PBS	
2a	2000 pg/mL CXCL8 plus 1000 ppm TiO_2 in PBS incubated for 1 h at room temperature then centrifuged at 800 ×*g* for 5 min	Supernatant
2b		TiO_2 pellet washed in PBS and re-suspended
3a	1000 ppm TiO_2 in PBS incubated for 1 h at room temperature then centrifuged at 800 ×*g* for 5 min	Supernatant
3b		TiO_2 pellet washed in PBS and re-suspended
4	2000 pg/mL CXCL8 in 20 % human serum	
5a	2000 pg/mL CXCL8 in 20 % human serum plus 1000 ppm TiO_2 in PBS incubated for 1 h at room temperature then centrifuged at 800 ×*g* for 5 min	Supernatant
5b		TiO_2 pellet washed in PBS and re-suspended

Neutrophil chemotaxis

Following informed consent (UK NRES 10/H1208/48), venous blood was collected in 6 mL Vacutainer™ (17 IU/mL heparin) anticoagulant tubes (Greiner, Stonehouse, UK) from volunteer donors (n = 14), 7 females and 7 males with a mean age of 27 ± 8 years (range: 20-45), who were not currently taking any anti-inflammatory or anti-microbial medication. The entire blood sample was layered gently over pre-prepared Percoll (GE Healthcare, Amersham, UK) gradients of 1.079 and 1.098 g/mL in a 25 mL centrifuge tube using a Pasteur pipette. Tubes were centrifuged for 8 min at 150 ×g followed immediately by 10 min at 1,200 ×g (Hettich Universal 320R, Hettich, Kirchlengern, Germany) to separate the neutrophil-containing layer, which was then aspirated prior to erythrocyte lysis using 0.83 % NH_4Cl containing 1 % $KHCO_3$, 0.04 % EDTA and 0.25 % BSA. Once isolated, the neutrophil pellet was resuspended in glucose and cation-supplemented PBS [Roswell Park Memorial Institute (RPMI) medium] at a concentration of 1 × 10^6 cells/mL. Cell viability was determined by trypan blue exclusion and was typically over 97 %.

An Insall chamber (Muinonen-Martin *et al.*, 2010) was used to allow quantitative imaging of neutrophil chemotaxis, according to methods

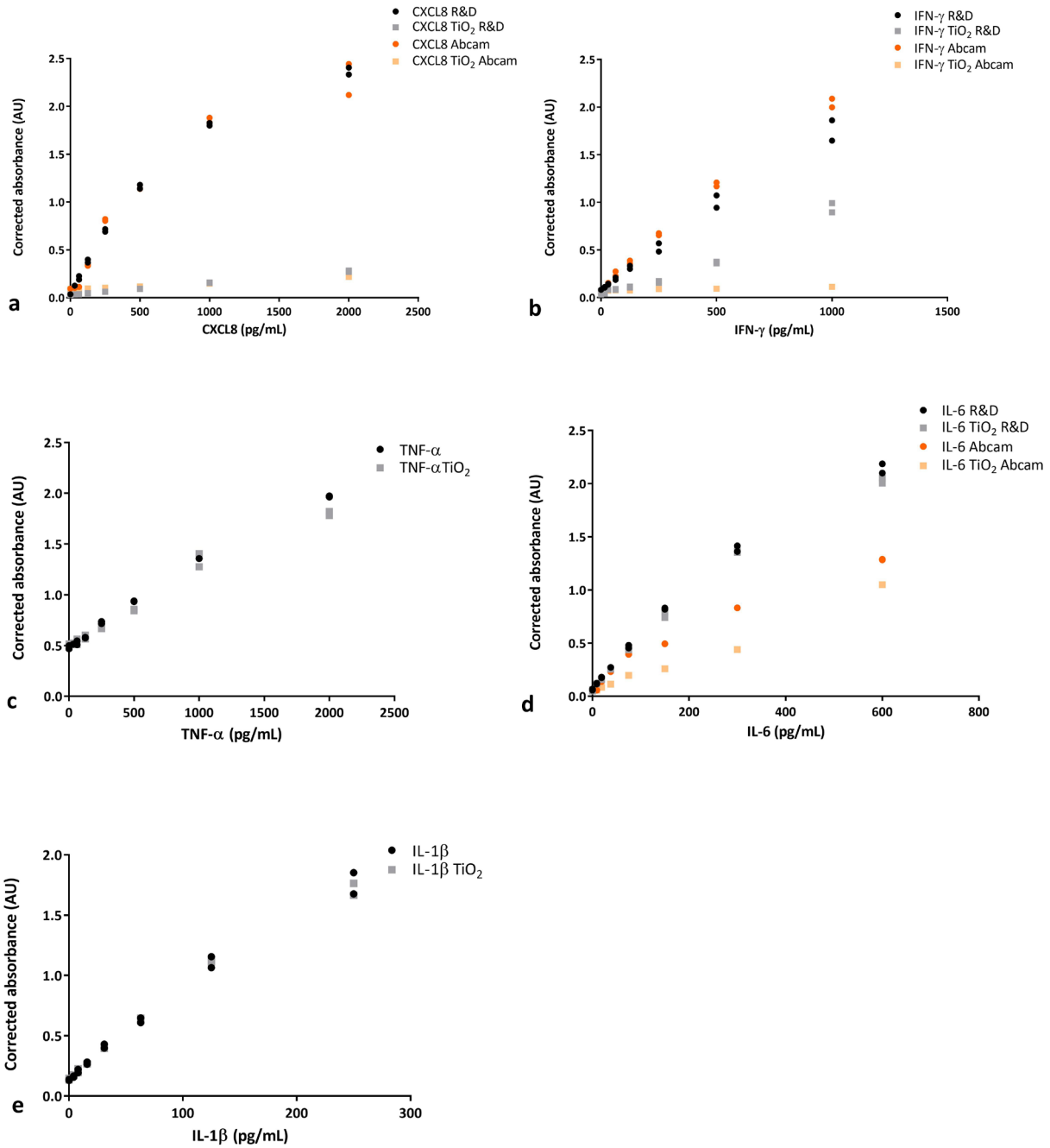

Fig. 2. (**a**-**e**) Plots of inflammatory mediators concentrations (replicate points shown) against absorbance (arbitrary units, AU) derived from ELISAs (n = 2 or n = 4) for the serially-diluted specific standard and for the serially-diluted specific standard following 24 h exposure to 100 ppm TiO_2 NPs and centrifugation to remove insoluble contents. Additional ELISA validation for CXCL8, IFN-γ and IL-6 (n = 4) were performed using R&D (grey/black) and Abcam (orange/yellow) assay kits.

described by Roberts *et al.*, (2015). Briefly, 22 mm coverslips (VWR International, Lutterworth, UK) were washed in 0.2 M HCl, dried and blocked using 7.5 % BSA (Sigma-Aldrich). Neutrophils, as prepared above (800 µL of ~ 1 × 10^6 cells/mL), were pipetted onto the coverslip and incubated at room temperature for 20 min to allow adherence. Then, the coverslip was inverted and placed carefully onto the Insall chamber (Fig. 1). Excess RPMI was absorbed from the edges of the coverslip to avoid flooding of the chamber and to allow the potential chemoattractant to be loaded into the bays. Following loading, the chamber was imaged every 30 s for 40 frames (20 min) using Q Imaging Retiga 2000R camera (Qimaging, Surry, Canada) attached to a Zeiss Primovert microscope (Carl Zeiss Imaging, Thormwood, NY, USA), allowing cell movement to be tracked. Control chemoattractants included RPMI (negative control), 10 nM N-Formylmethionyl-leucyl-phenylalanine (FMLP; positive control) and 200 ng/mL CXCL8 (positive control). To produce the experimental chemoattractants, 200 ng/mL CXCL8 was incubated for 1 h at room temperature with 100 ppm TiO_2 NPs, then centrifuged at 800 ×*g* for 5 min (Geneflow SciSPin Micro, Lichfield, UK) to produce an CXCL8 supernatant. The pellet was washed, then re-suspended in PBS-1 % BSA to produce a second chemoattractant. 100 ppm TiO_2 NPs suspended in PBS-1 % BSA formed the third chemoattractant (negative control). One video was captured using each potential chemoattractant per donor. Fig. 1 shows a diagram of the Insall chamber.

Quantitative analysis of chemotaxis

Analysis was performed according to methods described by Roberts *et al.*, (2015). Briefly, image frames were processed using the tracking plug-in of ImageJ 1.45SR software (National Institutes of Health, Bethesda, MD, USA), where a random selection of 15 cells in the image field of each video were tracked. Data gathered were used to calculate cell movement in terms of cell speed (movement per unit time in any direction), cell velocity (movement per unit time towards the chemoattractant) and chemotactic index (CI) – a measure of directional accuracy relative to the chemoattractant gradient (Andrew and Insall, 2007). XY co-ordinates of points from the videos were analysed using the CircStat toolbox (MATLAB; Mathworks, Natick, MA, USA) software to ascertain the significance of cell movement over time.

Protein gel electrophoresis

To further identify adsorption of CXCL8 to TiO_2 NPs and to ascertain any specificity of CXCL8 binding over other biomolecules, CXCL8 was exposed to TiO_2 NPs suspended in simple (BSA only, as before) and complex (human serum) media and protein gel electrophoresis was performed on centrifuge-separated supernatants and re-suspended TiO_2 particles. 12 % Bis-Tris protein gels (NuPAGE™ Novex™, Invitrogen, Paisley, UK) were employed and experimental samples prepared according to Table 1. 500 µL of each sample were concentrated using centrifuge filters (Amicon Ultra 0.5 mL 3K Ultracel, Millipore, Watford, UK) at 350 ×*g* for 30 min. Samples containing TiO_2 particles (Fig. 4, lanes 2b, 3b and 5b) were treated with reducing agent (50 mM dithiothreitol, NuPAGE® Sample Reducing Agent, Thermo Fisher Scientific, Loughborough, UK) and all samples were heated in sample buffer at 70 °C for 10 min prior to electrophoresis in 2-(N-morpholino) ethanesulfonic acid (MES) buffer (NuPAGE® MES SDS Running Buffer; Invitrogen) for 20 min. Following electrophoresis, the gel was stained for 1 h with Imperial Protein Stain (Thermo Fisher Scientific) according to manufacturer's instructions and washed in distilled water until the background was clear. Images were captured using a lightbox and a Canon S110 digital camera (Canon, Tokyo, Japan). See Table 1 for a complete list of prepared samples.

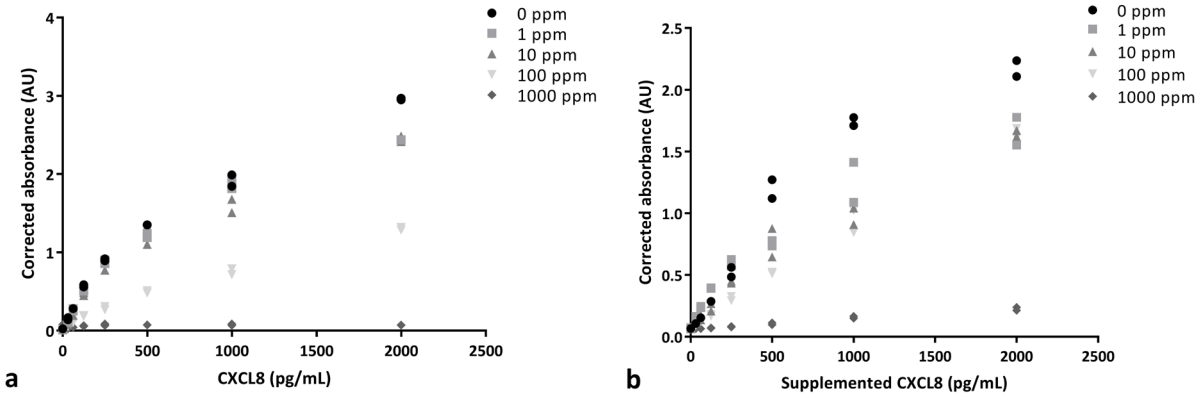

Fig. 3. Plots of CXCL8 mean concentration against absorbance (arbitrary units) derived from ELISAs (n = 3) of the CXCL8 standard (0 ppm) serially-diluted (1 in 10) in (**a**) standard reagent diluent and (**b**) human serum and for the CXCL8 standard following exposure to 1, 10, 100 and 1000 ppm of TiO_2 NPs for 1 h, then serially diluted in reagent diluent or human serum (1 in 10) before centrifugation to remove insoluble contents. Replicate data points shown (n = 2).

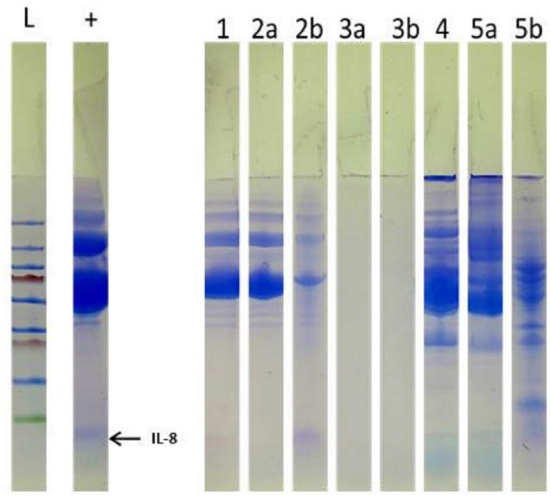

Fig. 4. Sections taken from an Imperial Protein Stain stained protein gel. Lane 1: 200 pg/mL CXCL8 in PBS (high standard used for the ELISA. The faint band is due to the low protein concentration used). Lane 2a: supernatant (SN) from 200 pg/mL CXCL8 in PBS plus 1000 ppm TiO_2 NPs incubated overnight, then centrifuged. Lane 2b: TiO_2 NPs centrifuged out from the sample in lane 2a, washed in PBS and resuspended prior to gel run. Lane 3: SN from TiO_2 NPs in PBS only, prepared as above. Lane 3b: TiO2 NPs centrifuged out and washed in PBS from the sample in lane 3a. Lane 4: 200 pg/mL CXCL8 in 20 % human serum and 80 % PBS. Lane 5a: SN from 200 pg/mL CXCL8 in 20 % human serum plus 1000 ppm TiO_2 NPs. Lane 5b: TiO_2 NPs centrifuged and washed in PBS from the sample in lane 5a. L = ladder, + = positive control (100 ng/mL CXCL8).

Results

Direct exposure of CXCL8 to TiO_2 NPs resulted in a strong and significant depletion in the absorbance signal, as detected at the end of the ELISA assay (Fig. 2**a**). A similar pattern of behaviour was observed with IF-γ, although the signal was not depleted as dramatically (Fig. 2**b**). However, exposure of TNFα, IL-1β and IL-6 to TiO_2 NPs resulted in no change to the ELISA data (Fig. 2**c**-**e**). These results suggested specificity in the interaction between TiO_2 and CXCL8 (and IF-γ).

To further investigate the interactions between CXCL8 and TiO_2 NPs, dose-dependency and dose-specificity of the binding were studied by titrating the concentration of TiO_2 NPs against the standard. Following NP exposure, NPs were separated by centrifugation as before. To further test the specificity of CXCL8 adsorption to the TiO_2 NPs, the NPs were pre-exposed to human serum to establish whether the avidity of the binding between CXCL8 and NPs was affected by other proteins present in tissue fluids *in vivo*.

Fig. 3**a**,**b** demonstrated a specific interaction between CXCL8 and TiO_2 NPs in terms of both a dose-dependent depletion and specificity in the presence of other serum proteins. To test further the specificity of binding between the TiO_2 NPs and CXCL8, protein gel electrophoresis was performed to identify proteins present within the samples when exposed to TiO_2. This technique will qualitatively demonstrate if any CXCL8 is bound to TiO_2 particles, once centrifuged, and if there is a depletion of CXCL8 signal in samples where the supernatant is tested post-centrifugation.

Samples showing the presence of CXCL8 were the positive control: lane 2b (where TiO_2 particles exposed previously to CXCL8 were separated by centrifugation and washed in PBS before electrophoresis) and lane 5b (where TiO_2 particles exposed previously to CXCL8 in 20 % human serum were separated by centrifugation and washed in PBS before electrophoresis) (Fig. 4). The results support ELISA data showing depletion of CXCL8 present in any supernatants where TiO_2 NPs were introduced and then removed by centrifugation. This strongly implied that the CXCL8 was bound to TiO_2 NPs and was removed from the supernatant during centrifugation. Subsequently, the functional consequences of CXCL8 depletion by TiO_2 NPs were considered by studying the chemotaxis of human PMNLs.

Fig. 5 and 6 showed the altered chemoattractant properties of CXCL8 once exposed to TiO_2 NPs. Fig. 7 and 8 demonstrated the loss of directional movement of PMNLs towards the supernatant remaining after the addition of TiO_2 NPs to CXCL8 and centrifugation to remove insoluble material, further indicating that the CXCL8 was bound to the NPs. Once the NPs were re-suspended, they did not act as a chemoattractant; therefore, indicating that the association with CXCL8 was robust. The chemotactic index and velocity shown in Fig. 7 and 8 demonstrated a dose-dependent reduction in movement of neutrophils towards the chemoattractant with increasing amounts of TiO_2 being present. Speed of PMNLs was not affected, suggesting that the random movement of cells remained consistent but directional accuracy of this movement was lost.

Discussion

The extracellular tissue compartment contains a wide variety of inflammatory mediators, which vary in composition and quantity in both health and disease (Dinarello, 2000; Zhang and An, 2007). Inflammatory mediator production and function is an essential part of the host's response to infection and injury (Soeters and Grimble, 2009; Zhang and An, 2007). The current study explored whether TiO_2 NPs could interfere with the bioavailability and function of the inflammatory mediators CXCL8, IFN-γ, IL-1β, TNFα and IL-6, which are released by the PMNLs and, therefore, are found at inflammatory sites where they could be exposed to the TiO_2 NPs. Due to its

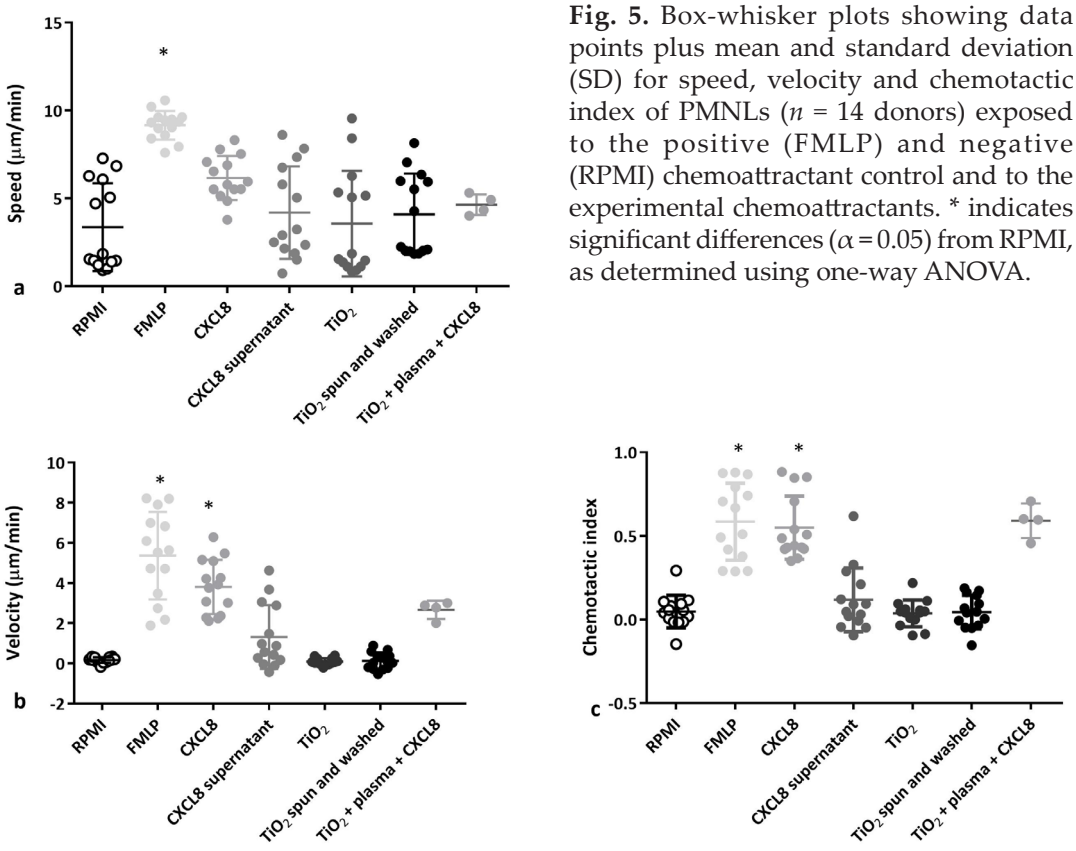

Fig. 5. Box-whisker plots showing data points plus mean and standard deviation (SD) for speed, velocity and chemotactic index of PMNLs (n = 14 donors) exposed to the positive (FMLP) and negative (RPMI) chemoattractant control and to the experimental chemoattractants. * indicates significant differences ($\alpha = 0.05$) from RPMI, as determined using one-way ANOVA.

chemotactic properties, there was considerable focus on the chemokine CXCL8. Humans are exposed to a wide variety of NPs and specifically to TiO_2 NPs through gastrointestinal absorption, dermal exposure and from implanted Ti biomedical devices, where *in situ* generation and accumulation of TiO_2 NPs in adjacent tissues is demonstrated (Batt, 2017). The current study explored one tetragonal crystalline form of TiO_2 (anatase), which is present in inflamed tissues surrounding Ti implanted devices (Addison *et al.*, 2012).

The high surface adsorption energy of NPs is due to their large surface to volume ratio. NPs surfaces present a large number of unsaturated chemical bonds with which biomolecules can interact (Xia *et al.*, 2011). Therefore, biological characterisation of NPs is complicated by adsorption of proteins and biomolecules to their surfaces, a process which is competitive and highly dynamic dependent upon environmental perturbations (Xia *et al.*, 2011). Current opinion is that, in biological media, NPs form a corona made up of a strongly bound monomolecular layer of small molecules and plasma proteins attached to their surfaces, with more loosely adsorbed biomolecules attached, which can be exchanged with the environment (Cedervall *et al.*, 2007; Lynch *et al.*, 2006). However, the physical and chemical factors that govern these interactions remain poorly understood. In an attempt to further understanding, Xia and co-workers develop a biological surface adsorption index and identify that, in comparison with carbon nanomaterials, TiO_2 NPs are predicted to weakly adsorb to biomolecules (Xia *et al.*, 2010).

In this study, it was demonstrated that there was selectivity in the interactions between the inflammatory mediators CXCL8, IF-γ, IL-1β, TNFα, IL-6 and the TiO_2 NPs when directly exposed to each other (in the presence of BSA), with significant reductions in the ELISA signal data for CXCL8 and to a lesser extent IFN-ɣ, when compared to other pro-inflammatory mediators. A clear exposure concentration dependency was observed for CXCL8 adsorption to TiO_2 NP surfaces rather than interference with other components of the ELISA assay. Exposure of CXCL8 to TiO_2 NPs in the more complex human serum medium resulted in the same pattern of observations as the direct exposure to CXCL8 and suggested (although not empirically demonstrated) that CXCL8 was strongly and selectively adsorbed and did not form a weakly adsorbed biomolecular corona. Supporting data were generated from the electrophoretic separation of CXCL8 and TiO_2 NPs, with CXCL8 only detectable on the separated NPs, with no significant signal in the remaining medium. To demonstrate whether the CXCL8 remained bio-available (hence providing further information regarding strength of adsorption to the NPs), functional assays were performed with TiO_2 NP exposures in biologically-relevant media. CXCL8 is important for PMNL chemotaxis and it was demonstrated to act strongly as a PMNL chemoattractant, resulting in a significant increase

in chemotactic velocity and chemotactic index in the Insall chamber assay. Subsequently, TiO_2 NP addition to CXCL8 eliminated the differences in PMNL movement in a dose-responsive pattern, when compared with the negative control, suggesting a dilution of the CXCL8 gradient across the assay measurement bridge.The CXCL8 exposed TiO_2 NPs also demonstrated no chemoattractant properties, indicating again that CXCL8 was strongly adsorbed. Given the clear association with CXCL8, these findings suggested that the null hypothesis, according to which the presence of TiO_2 NPs had no selective impact on extracellular inflammatory mediator adsorption, should be rejected.

The potential of TiO_2 NPs to stimulate CXCL8 production in human cell lines is documented; however, ELISA techniques are employed to identify CXCL8 concentrations (Haleem-Smith *et al.*, 2012; Wilson *et al.*, 2012). The current study demonstrated that ELISA measurement of CXCL8 in the presence of TiO_2 NPs was unreliable due to the strong adsorption of CXCL8 to TiO_2 NPs. Although TiO_2 NPs are described as weak adsorbers (Xia *et al.*, 2011), the dominant variable affecting TiO_2 NPs ability to bind biomolecules is the particle size (Horie *et al.*, 2013). Increasing particle size decreases the surface to volume ratio of the particle, affecting its capacity to adsorb biomolecules to its surface. It should be noted that the TiO_2 NPs used in the present study agglomerated to some extent once introduced into BSA-containing reagent diluent (or human serum), but that the CXCL8 binding was not impeded.

The accumulation of insoluble TiO_2 is demonstrated in a number of tissues, including lungs and peri-implant tissues, where there may be simultaneous infection and/or inflammation (Batt, 2017; Deppe *et al.*, 2002; Fretwurst *et al.*, 2016; Passi *et al.*, 2002). The results of this study suggested that the TiO_2 NPs accumulated in discrete regions could preferentially adsorb CXCL8 (and IFN-γ), despite the presence of other biomolecules and, thereby, modify local inflammatory mediator concentrations. In a three-dimensional tissue space, a localised reduction of CXCL8 concentration by TiO_2 NPs would modify (potentially reversing completely) the chemoattractant gradients, leading to disrupted movement of PMNLs within the tissues, thereby delaying bacterial clearance and resolution of inflammation. CXCL8 also induces processes important in host defences, such as phagocytosis. Therefore, the presence of TiO_2 NPs would lead to localised regions where clearance of microbes

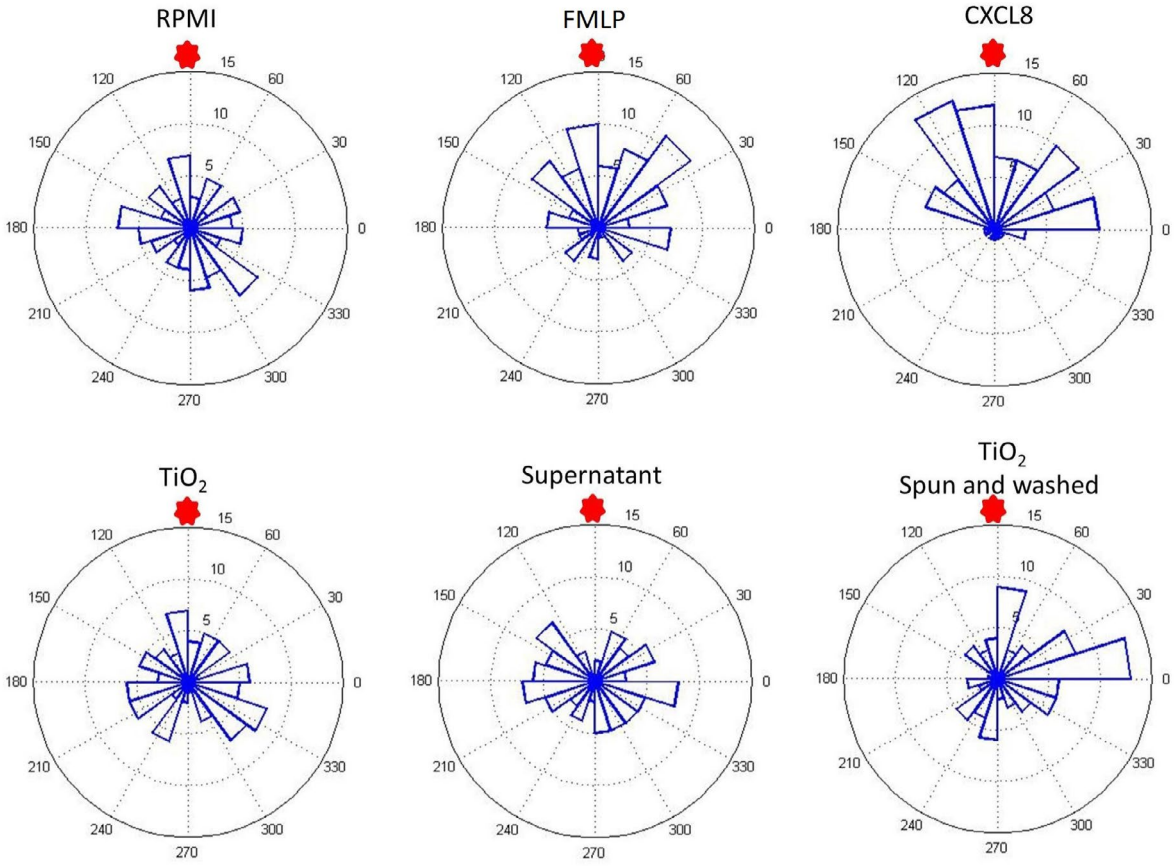

Fig. 6. Chemotaxis vector plots showing the proportion and directionality of movement of cells in each segment during the observation period. The larger the segment, the more cells moved preferentially in that direction. The inner numerical notation shows radially the distance moved and the circumferential numerical notation the movement angle, where the chemoattractant gradient is normally to 90° (indicated by star annotation). Clear directional movement towards the chemoattractant was observed for FMLP and CXCL8 by the more vertical direction of the segments.

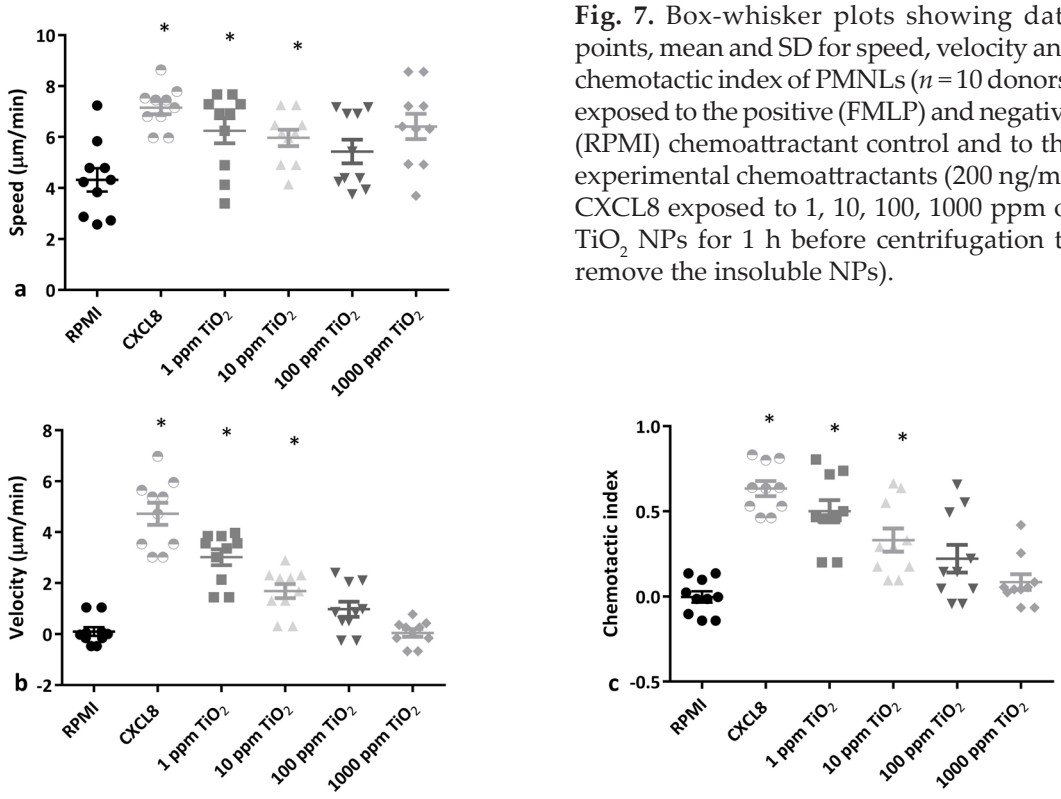

Fig. 7. Box-whisker plots showing data points, mean and SD for speed, velocity and chemotactic index of PMNLs ($n = 10$ donors) exposed to the positive (FMLP) and negative (RPMI) chemoattractant control and to the experimental chemoattractants (200 ng/mL CXCL8 exposed to 1, 10, 100, 1000 ppm of TiO_2 NPs for 1 h before centrifugation to remove the insoluble NPs).

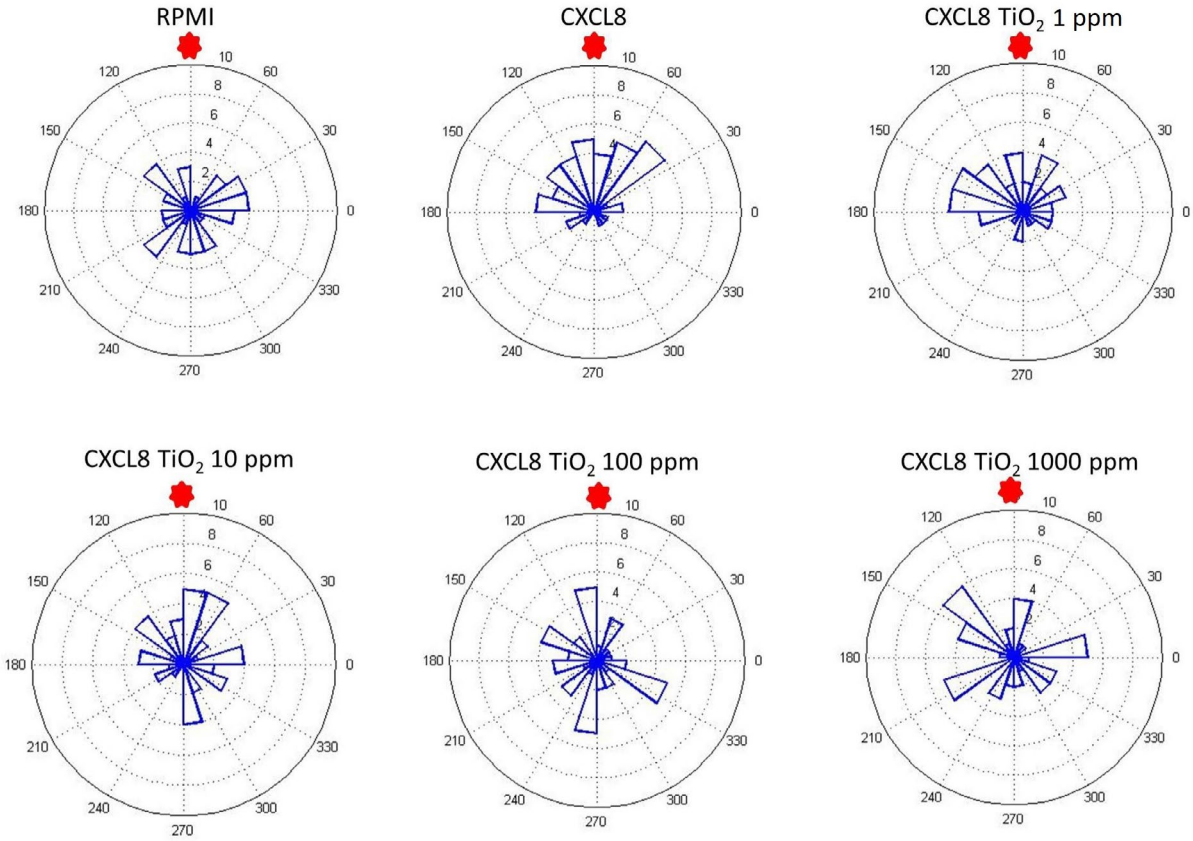

Fig. 8. Chemotaxis vector plots showing the proportion and directionality of movement of cells in each segment during the observation period. The inner numerical notation shows radially the distance moved and the circumferential numerical notation the movement angle, where the chemoattractant gradient is normally to 90° (indicated by star annotation). Clear directional movement towards the chemoattractant is observed for FMLP and for CXCL8. However, > 1 ppm TiO_2 exposure resulted in non-preferential directional movement.

and cellular debris is compromised. The observed depletion of IFN-γ requires further investigation. IFN-γ can initially down-regulate the expression of CXCL8 by PMNLs, whilst up-regulating the expression of the pro-inflammatory inflammatory mediators IL-1β and TNFα (Ellis and Beaman, 2004). IFN-γ also supresses chemotactic migration of PMNLs towards FMLP and it is postulated that these behaviours indicate that IFN-γ can signal to the PMNLs the arrival at the site of inflammation (Ellis and Beaman, 2004). A potential consequence of TiO_2 NP binding would again be a disruption in the arrival of PMNLs at the injured site. Furthermore, PMNL hyper-reactivity is reported in several chronic inflammatory diseases such as periodontitis (Matthews *et al.*, 2007). Therefore, further disruption of chemotactic accuracy and velocity of neutrophils could increase tissue transit times and, thus, potentiate PMNL-mediated collateral tissue damage in susceptible patients.

Conclusions

TiO_2 NPs localise within inflamed peri-implant tissues associated with Ti devices. The perturbation of CXCL8 activity as a consequence of binding to TiO_2 NPs might be a modifying factor in disease processes, such as dental peri-implantitis, where there is chronic inflammation of the peri-implant tissues. Whilst this study demonstrated the interaction between TiO_2 NPs and CXCL8, IFN-γ also appeared to selectively bind to TiO_2 NPs, but to a lesser extent. Other cytokines may show similar behaviour and further investigations are required.

Acknowledgements

O. Addison was funded by the UK National Institute for Health Research award NIHR/CS/010/001. This article presents independent research funded by the National Institute for Health Research (NIHR). The views expressed are those of the author(s) and not necessarily those of the NHS, the NIHR or the Department of Health.

References

Addison O, Davenport AJ, Newport RJ, Kalra S, Monir M, Mosselmans JF, Proops D, Martin RA (2012) Do 'passive' medical titanium surfaces deteriorate in service in the absence of wear?. J R Soc Interface **9**: 3161-3164.

Andrew N, Insall RH (2007) Chemotaxis in shallow gradients is mediated independently of PtdIns 3-kinase by biased choices between random protrusions. Nat Cell Bio **9**: 193-200.

Batt J (2017) The biological effects of titanium corrosion products on gingival epithelium. PhD thesis. School of Dentistry, University of Birmingham. ID code: 7810.

Bickel M (1993) The role of interleukin-8 in inflammation and mechanisms of regulation. J Periodontol **64**: 456-60.

Bonner JC, Silva RM, Taylor AJ, Brown JM, Hilderbrand SC, Castranova V, Porter D, Elder A, Oberdorster G, Harkema JR, Bramble LA, Kavanagh TJ, Botta D, Nel A, Pinkerton KE (2013) Interlaboratory evaluation of rodent pulmonary responses to engineered nanomaterials: the NIEHS Nano GO Consortium. Environ Health Perspect **121**: 676-682.

Brun E, Barreau F, Veronesi G, Fayard B, Sorieul S, Chaneac C, Carapito C, Rabilloud T, Mabondzo A, Herlin-Boime N, Carriere M (2014) Titanium dioxide nanoparticle impact and translocation through *ex vivo*, *in vivo* and *in vitro* gut epithelia. Part Fibre Toxicol **11**: 13.

Cadosch D, Chan E, Gautschi OP, Simmen HP, Filugueira L (2009) Bio-corrosion of stainless steel by osteoclasts-in vitro evidence. J Orthop Res **27**: 841-846.

Cedervall T, Lynch I, Lindman S, Berggard T, Thulin E, Nilsson H, Dawson KA, Linse S (2007) Understanding the nanoparticle-protein corona using methods to quantify exchange rates and affinities of proteins for nanoparticles. Proc Natl Acad Sci U S A **104**: 2050-2055.

Chan J, Ying T, Guang YF, Lin LX, Kai T, Fang ZY, Ting YX, Xing LF, Ji YY (2011) *In vitro* toxicity evaluation of 25-nm anatase TiO2 nanoparticles in immortalized keratinocyte cells. Biol Trace Elem Res **144**: 183-196.

Dinarello CA (2000) Proinflammatory cytokines. Chest **118**: 503-508.

Ellis TN, Beaman BL (2004) Interferon-γ activation of polymorphonuclear neutrophil function. Immunol **112**: 2-12.

Elgrabli D, Beaudouin R, Jbilou N, Floriani M, Pery A, Rogerieux F, Lacroix G (2015) Biodistribution and clearance of TiO2 nanoparticles in rats after intravenous injection. PloS One **10**: e0124490.

Frohlich E, Roblegg E (2012) Models for oral uptake of nanoparticles in consumer products. Toxicol **291**: 10-17.

Gerloff K, Fenoglio I, Carella E, Kolling J, Albrecht C, Boots AW, Forster I, Schins RP (2012) Distinctive toxicity of TiO2 rutile/anatase mixed phase nanoparticles on Caco-2 cells. Chem Res Toxicol **25**: 646-655.

Gurr JR, Wang AS, Chen CH, Jan KY (2005) Ultrafine titanium dioxide particles in the absence of photoactivation can induce oxidative damage to human bronchial epithelial cells. Toxicol **213**: 66-73.

Haleem-Smith H, Argintar E, Bush C, Hampton D, Postma WF, Chen FH, Rimington T, Lamb J, Tuan RS (2012) Biological responses of human mesenchymal stem cells to titanium wear debris particles. J Orthop Res **30**: 853-863.

Holpuch AS, Hummel GJ, Tong M, Seghi GA, Pei P, Ma P, Mumper RJ, Mallery SR (2010) Nanoparticles

for local drug delivery to the oral mucosa: proof of principle studies. Pharm Res **27**: 1224-1236.

Horie M, Kato H, Iwahashi h (2013) Cellular effects of manufactured nanoparticles: effect of adsorption ability of nanoparticles. Arch Toxicol **87**: 771-781.

Hsiao IL, Huang YJ (2011) Improving the interferences of methyl thiazolyl tetrazolium and IL-8 assays in assessing the cytotoxicity of nanoparticles. J Nanosci Nanotechnol **11**: 5228-5233.

Irshad M, Scheres N, Crielaard W, Loos BG, Wismeijer D, Laine ML (2013) Influence of titanium on *in vitro* fibroblast-Porphyromonas gingivalis interaction in peri-implantitis. J Clin Periodontol **40**: 841-849.

Jani P, Halbert GW, Langridge J, Florence AT (1990) Nanoparticle uptake by the rat Gastrointestinal mucosa: quantitation and particle size dependency. J Pharm Pharmacol **42**: 821-826.

Jani PU, Mccarthy DE, Florence AT (1994) Titanium-dioxide (Rutile) particle uptake from the rat GI tract and translocation to systemic organs after oral-administration. International J Pharm **105**: 157-168.

Jin C, Tang Y, Yang FG, Li XL, Xu S, Fan XY, Huang YY, Yang YJ (2011) Cellular toxicity of TiO2 nanoparticles in anatase and rutile crystal phase. Biol Trace Elem Res **141**: 3-15.

Jonas L, Fulda G, Radeck C, Henkel KO, Holzhüter G, Mathieu HJ (2001) Biodegradation of titanium implants after long-time insertion used for the treatment of fractured upper and lower jaws through osteosynthesis: element analysis by electron microscopy and EDX or EELS. Ultrastruct Pathol **25**: 375-383

Kobayashi N, Naya M, Endoh S, Maru J, Yamamoto K, Nakanishi J (2009) Comparative pulmonary toxicity study of nano-TiO(2) particles of different sizes and agglomerations in rats: different short- and long-term post-instillation results. Toxicol **264**: 110-118.

Kocbek P, Teskac K, Kreft ME, Kristl J (2010) Toxicological aspects of long-term treatment of keratinocytes with ZnO and TiO2 nanoparticles. Small **6**: 1908-1917.

Kroll A, Pillukat MH, Hahn D, Schnekenburger J (2009) Current *in vitro* methods in nanoparticle risk assessment: limitations and challenges. Eur J Pharm Biopharm **72**: 370-377.

Lu J, Rao MP, MacDonald NC, Khang D, Webster TJ (2008) Improved endothelial cell adhesion and proliferation on patterned titanium surfaces with rationally designed, micrometer to nanometer features. Acta Biomater **4**: 192-201.

Lynch I, Dawson KA, Linse S (2006) Detecting cryptic epitopes created by nanoparticles. Sci STKE **2006**: pe14.

Matthews JB, Wright HJ, Roberts A, Ling-Mountford N, Cooper PR, Chapple IL (2007) Neutrophil hyper-responsiveness in periodontitis. J Dent Res **86**: 718-722.

Monteiro-Riviere NA, Inman AO (2006) Challenges for assessing carbon nanomaterial toxicity to the skin. Carbon **44**: 1070-1078.

Muinonen-Martin AJ, Veltman DM, Kalna G, Insall RH (2010) An improved chamber for direct visualisation of chemotaxis. PLoS One **5**: e15309.

Olmedo DG, Duffó G, Cabrini RL, Guglielmotti MB (2008) Local effect of titanium implant corrosion: an experimental study in rats. Int J Oral Maxillofac Surg **37**: 1032-1038.

Park EJ, Yi J, Chung KH, Ryu DY, Choi J, Park K (2008) Oxidative stress and apoptosis induced by titanium dioxide nanoparticles in cultured BEAS-2B cells. Toxicol Lett **180**: 222-229.

Peters K, Unger RE, Kirkpatrick CJ, Gatti AM, Monari E (2004) Effects of nano-scaled particles on endothelial cell function *in vitro*: studies on viability, proliferation and inflammation. J Mater Sci Mat Med **15**: 321-325.

Qian Y, Zhang XL, Zeng BF, Jiang Y, Shen H, Wang Q (2013) Substance P enhanced titanium particles-induced RANKL expression in fibroblasts from periprosthetic membrane. Connect Tissue Res **54**: 361-366.

Roberts HM, Ling MR, Insall R, Kalna G, Spengler J, Grant MM, Chapple IL. (2015) Impaired neutrophil directional chemotactic accuracy in chronic periodontitis patients. J Clin Periodontol **42**: 1-11.

Shukla RK, Kumar A, Pandey AK, Singh SS, Dhawan A (2011) Titanium dioxide nanoparticles induce oxidative stress-mediated apoptosis in human keratinocyte cells. J Biomed Nanotechnol **7**: 100-101.

Silva RM, Teesy C, Franzi L, Weir A, Westerhoff P, Evans JE, Pinkerton KE (2013) Biological response to nano-scale titanium dioxide (TiO2): role of particle dose, shape, and retention. J Toxicol Environ Health A **76**: 953-972.

Singh S, Shi T, Duffin R, Albrecht C, van Berlo D, Hohr D, Fubini B, Martra G, Fenoglio I, Borm PJ, Schins RP (2007) Endocytosis, oxidative stress and IL-8 expression in human lung epithelial cells upon treatment with fine and ultrafine TiO2: role of the specific surface area and of surface methylation of the particles. Toxicol Appl Pharmacol **222**: 141-151.

Soeters PB, Grimble RF (2009) Dangers, and benefits of the cytokine mediated response to injury and infection. Clin Nutr **28**: 583-596.

Srivastava RK, Rahman Q, Kashyap MP, Singh AK, Jain G, Jahan S, Lohani M, Lantow M, Pant AB (2013) Nano-titanium dioxide induces genotoxicity and apoptosis in human lung cancer cell line, A549. Hum Exp Toxicol **32**: 153-166.

Taurozzi JS, Hackley VA, Wiesner MR (2013) A standardised approach for the dispersion of titanium dioxide nanoparticles in biological media. Nanotoxicol **7**: 389-401.

Tenzer S, Docter D, Kuharev J, Musyanovych A, Fetz V, Hecht R, Schlenk F, Fischer D, Kiouptsi K, Reinhardt C, Landfester K, Schild H, Maskos M,

Knauer SK, Stauber RH (2013) Rapid formation of plasma protein corona critically affects nanoparticle pathophysiology. Nat Nanotechnol **8**: 772-781.

Torgersen S, Gjerdet NR, Erichsen ES, Bang G (1995) Metal particles and tissue changes adjacent to miniplates. A retrieval study. Acta Odontol Scand **53**: 65-71.

Tucci P, Porta G, Agostini M, Dinsdale D, Iavicoli I, Cain K, Finazzi-Agro A, Melino G, Willis A (2013) Metabolic effects of TiO_2 nanoparticles, a common component of sunscreens and cosmetics, on human keratinocytes. Cell Death Dis **4**: e549.

Veranth JM, Kaser EG, Veranth MM, Koch M, Yost GS (2007) Cytokine responses of human lung cells (BEAS-2B) treated with micron-sized and nanoparticles of metal oxides compared to soil dusts. Part Fibre Toxicol **4**: 2.

Wilson D, Zaqout M, Heo JH, Park EK, Oak CH, Ueno S (2012) Nuclear factor-kappa B is not involved in titanium dioxide-induced inflammation. J UOEH **34**: 183-191.

Wilson MR, Stone V, Cullen RT, Searl A, Maynard RL, Donaldson K (2000) *In vitro* toxicology of respirable Montserrat volcanic ash. Occup Environ Med **57**: 727-733.

Xia XR, Monteiro-Riviere NA, Mathur S, Song XF, Xiao LS, Oldenberg SJ, Fadeel B, Riviere JE (2011) Mapping the surface adsorption forces of nanomaterials in biological systems. ACS Nano **5**: 9074-9081.

Xia XR, Monteiro-Riviere NA, Riviere JE (2010) An index for characterization of nanomaterials in biological systems. Nat Nanotechnol **5**: 671-675.

Yazdi AS, Guarda G, Riteau N, Drexler SK, Tardivel A, Couillin I, Tschopp J (2010) Nanoparticles activate the NLR pyrin domain containing 3 (Nlrp3) inflammasome and cause pulmonary inflammation through release of IL-1 α and IL-1β. Proc Natl Acad Sci U S A **107**: 19449-19454.

Yin ZF, Wu L, Yang HG, Su YH (2013) Recent progress in biomedical applications of titanium dioxide. Phys Chem Chem Phys **15**: 4844-4858.

Zhang JM, An J (2007) Cytokines, inflammation, and pain. Int Anesthesiol Clin **45**: 27-37.

Zhang LW, Monteiro-Riviere NA (2013) Use of confocal microscopy for nanoparticle drug delivery through skin. J Biomed Opt **18**: 061214.

Zhang W (2014) Nanoparticle aggregation: principles and modeling. Adv Exp Med Biol **811**: 19-43.

Discussion with Reviewer

Fackson Mwale: TiO_2 NPs stimulate CXCL8 upon human neutrophils activation. Does this effect decrease as TiO_2 is bound to CXCL8?
Authors: TiO_2 NPs exposure to human neutrophils results in a number of inflammatory events, including reactive oxygen species (ROS) generation, neutrophil extra-cellular trap (NET) formation and release of pro-inflammatory cytokines, including CXCL8. Quantification of CXCL8 release is routinely reported using ELISA techniques. This study suggested that the detected CXCL8 might have been underestimated in previous TiO_2 NP exposure studies. *In vivo*, the presence of TiO_2 NPs might reduce the levels of physiologically-available CXCL8.

Fackson Mwale: What is the impact of these studies in terms of clinical translation?
Authors: Our mechanistic understanding of materials determinants of peri-implant inflammation is not fully understood. Generation of nano-scale particles following tribocorrosion or mechanically-assisted corrosion of metallic implants occurs for a wide range of devices. To date, the major focus is on how such debris interacts with cellular components of the immune response. Here, it was demonstrated that TiO_2 NPs, which have been detected in peri-implant tissues associated with dental, craniofacial and orthopaedic devices, might exert a more subtle influence on peri-implant inflammation, by extracellular interactions with signalling molecules involved in immune cell recruitment and function.

Fackson Mwale: What are the mechanisms involved in CXCL8 depletion and how would you envisage tackling the problem of generated TiO_2 NPs?
Authors: We agree that these questions are important and future work will concentrate on answering them. However, we believe that the investigation into these mechanisms will be wide ranging and that the scope of this study was to highlight and describe the interaction along with the potential effects that there might be experimentally and clinically.

Editor's note: The Scientific Editor responsible for this paper was Mauro Alini.